Eng. & Tech. Journal, Vol.29, No.15, 2011

Improvement of Ballast Embankment Resting on Soft Clay by Reed and Asphalt Layers

Dr. Namir.K.S. AL-Saoudi*, Dr.Falah.H.Rahil* & Kawther.Y.H.AL-Soudany*

Received on: 30/6 /2011
Accepted on: 3/11 /2011

Abstract

The present paper investigates the possibility of using reed and /or asphalt as stabilizing materials for ballast model embankment overlaying a bed of soft soil. Four model tests were performed consisting of a model embankment 500mm base width 300mm crest width and 75mm high. The embankment was constructed on a bed of saturated soft clay 500mm thick with undrained shear strength 16 kPa. The ballast embankment was gradually loaded up to failure by a model footing 200mm wide and 400mm long placed on the crest with continuous monitoring of the generated settlement. The use reed and/or asphalt along the interface surface between the ballast embankment and the soft soil demonstrated significant improvements in both load carrying capacity and reduction in settlement.

Keywords: Reed, ballast embankment, soft clay, improvement

تحسين كفاءة السده الحجريه المنشأة على تربه طينيه باستخدام طبقات القصب والاسفلت

الخلاصة

يتحرى البحث عن امكانية استخدام القصب والاسفلت كمواد مثبته لموديل سده حجريه تستقر على طبقه ضعيفه . لذلك تم تحضير اربع موديلات يتألف كل موديل منها من سده حجريه ذات قاعدة سفلى عرضها500مم وقاعدة عليا عرضها 300مم وذات ارتفاع 75مم . وقد نفذت السده على تربه طينيه ضعيفه مشبعه سمكها 500مم ومقاومة قص الغير مبزوله لها 16كيلو باسكال.

تم تحميل موديل السده الحجريه بشكل تدريجي لحين الوصول للفشل باستخدام اساس عرضه 200مم وطوله 400مم استند على القاعدة العليا للسدة وتم مراقبة الهبوط الحاصل بشكل مستمر. ان استخدام القصب مع الاسفلت او بدونه عند الخط الفاصل بين السده الحجريه والتربه الضعيفة أعطى تحسنا" ملحوظا" لكل من قابلية التحمل ونقصان في الهبوط.

1. Introduction

Both reed and asphalt are abundant natural materials in Iraq, historically the two materials were used for many construction purposes. Reed usually is reformed in special structural element to construct small houses as the case in the marshes area south of Iraq. Also Iraqis were the first to use Reed in the form of sheets inter bedded between the earth as a Reinforcement in Aqarquf Zakurat about 1400 year B.C.

There are many other events where asphalt incorporated with stone in the form of columns was found underneath many ancient structures in many parts of Iraq. Like Ur (Wooley, 1926). Other natural materials such as nonwood plant fiber like plam leaves, reed and

* Building and Construction Engineering Department, University of Technology/ Baghdad

bamboo are also proposed as additional building units (Mwasha, 2009, Abbawi, 2002, Kadir, 1990, Al-Sudani,1988, Ambroziak,1968, Badanoiu, and Oradeanu, 1958).

The current study is an attempt to model the behavior of ballast model embankment constructed on a layer of soft clay with reed and/ or asphalt used along the interface surface between the two materials. Details are outlined in the following sections.

2. Experimental work

2.1 Model Tests

The experimental work consists of four model tests as shown in table (1) with the following details.

1. Model No.1 represents a ballast model embankment resting on a bed of soft clay of c_u=16 kN/m^2 without any treatment.
2. Model No.2 was performed with two layers of reed placed in perpendicular direction along the interaction surface between the ballast model embankment and the soft soil.
3. Model No.3 similar to the model No.2 with a layer of asphalt between the two reed layers.
4. Model No.4 similar to model No.3 with additional asphalt layer spread on the top surface of the reed layer.

2.2 Materials Used

2.2.1 The Soil used

Brown clayey soil was brought from Baldroze site about (60) kM east of Baghdad. The soil consists of 3.3 % sand, 31.7% silt and 65% clay. According to USCS, the soil is classified as CL. Details of the physical and chemical properties are outline in table (2).

2.2.2 The Crushed Stone

The crushed stone materials were obtained from a crushing stone factory. It is produced as a result of crushing big stones brought from Penjwen city located in northern part of Iraq. The crushed stone is of white colour and has angular shape. The crushed stone is of a uniform size, according to the coefficients of uniformity and curvature shown in table (3) the material was considered as poorly graded. Other physical properties are also shown in table (3).

2.2.3 Reed

Reed is an abundant natural material available in the southern part of Iraq, particularly in marshes area. The diameter of reed used in this research ranges from (8-16mm). Simple compression test was performed to determine the relationship between the stresses at failure versus diameter of reed which revealed the relationship shown in figure (1).

2.2.4 Asphalt

The asphalt used was grade (40-50) known as (Asphalt Cement) obtained from Al-Dora Refinery. Physical properties of the Asphalt Cement are shown in table (4).

2.3 Model Preparation and Testing

2.3.1 Preparation Bed of Soil

The bed of soil was prepared at liquidity index 0.3 revealing an undrained shear strength Cu=16 kN/m^2. This number was selected as a representative of most soft saturated soils located in the middle and southern parts of Iraq. Each 25 kg of natural soil was mixed with corresponding quantity of water to provide the desired undrained shear strength. After thorough mixing, the wet soil was kept inside tightened polythen bags for a period of two days to get uniform moisture content. The soil was placed in ten layers inside a steel container of 1000 $\times$400$\times$700 mm in depth. Each layer was compacted gently with a wooden tamper of size 75 mm $\times$ 75 mm in order to remove entrapped. After completing the final layer, the top surface was scraped and leveled surface then covered with polythen sheet to prevent any loss of moisture. A wooden board of similar area to that of the surface area of bed soil was placed on the bed then a setting pressure of 5 kPa was applied. The bed was left for a period of two days to regain part of its strength. The ballast embankment and/or the reed and asphalt layers were then placed as demonstrated in table (1). A footing 200mm wide and 400mm long was then placed on the crest of the embankment and loaded by a compression stress at a constant rate up to failure. The generated settlement was recorded at time intervals during the loading process. At the end of the test the front side of the steel container was disabled and photos of the deformed sections were taken.

3. Presentation and Discussions of Results

The results of the four model tests are presented and discussed in terms of bearing ratio defined as the ratio of the applied stress to the undrained shear strength, denoted by q/c_u, plotted against settlement ratio defined as the ratio of the generated settlement to the width of the footing and denoted by S/B. Figures 2, 3, 4 and 5 demonstrate the results of the four model tests. Each figure contains three curves representing the measured total generated settlement in the two layers, in addition to the calculated settlements in both ballast and clay layers. To determine the contribution of each layer in the total generated settlement, the settlement in the clay layer was calculated according to the following equation (Bowels, 1996).

$$S = \frac{\mu \;\; * \mu_1 * \Delta q * B}{E}$$

Where:

μ , μ_1: Coefficients for immediate settlement under a flexible foundation.

Δq: Applied stress.

B: Width of the footing.

E: Modulus of elasticity.

The application of this equation is accepted since the model tests were performed in short period less than 1.5 hour and then undrained conditions were valid.

Accordingly the following values are used

μ = 0.95

μ_1 = 0.6

B = 200mm

E = 1625kN/m^2 obtained from load settlement relationship of a model test performed on saturated bed clay at c_u= 16kN/m^2.

Figure 2 represents the results of model No.1, using ballast layer only without any additional materials along the interface surface between the clay layer and the ballast layer. This model is considered as the reference test to the other three tests.

Considering failure as the bearing ratio corresponding to 10% settlement ratio defined as 10% of the footing width depending on the proposal given by (Terzaghi 1967). The bearing ratio at failure is $(q/c_u)_f = 5.8$ and the corresponding settlement ratio for the clay and ballast layers are 2% and 8% respectively. It is worth mentioning that the settlement ratio of the clay to the settlement ratio of the ballast is 1/4. The bearing ratio at failure of deducted from this model test is considered as a benchmark for comparison purposes with other model tests. Figure 3 demonstrates the results of the model test No.2 with two layers of reed placed along the interface surface between the ballast and clay layers. The figure clearly shows that the presence of two layers of reed had substantial contribution in reducing the generated settlement at any stage of stress level. At bearing ratio 5.8 which is the bearing ratio at failure for the untreated model test, the total settlement ratio is 4.9 and the settlement ratio corresponding to the clay and ballast layers are 2 and 2.9 respectively, indicating a proportionality ratio 2/2.29 = 1/1.45. The bearing ratio at failure for this particular model test q/c_u = 9.6 corresponding to deformation ratio S/B = 10%. The applied stress was extended beyond failure and crushing of reed was noticed at $q/c_u \approx 12$ accompanied by substantial increase in the rate of settlement. It can be stated that the major reduction in settlement due to the presence of reed layer occurred in the ballast layer. The factor of safety for this model is equal to 9.6/5.8 = 1.66.

In model test No.3, the same two layers of reed were used in addition to asphalt layer in between. The bearing ratio versus settlement ratio, figure 4, demonstrated a bearing ratio at failure $(q/c_u)_f = 11.8$. At this bearing stress the settlement ratio of the clay and ballast layers are 4% and 6% respectively. The post failure stage demonstrates gradual increase in the rate of settlement up to $q/c_u \approx 15$, followed by a sharp increase in settlement. Regarding the working stress conditions, at $q/c_u = 5.8$, the corresponding total settlement ratio $(S/B)_{clay}$ and $(S/B)_{ballast}$ being 2 and 1 respectively as shown in table (5). The reduction in settlement as compared with corresponding results from model test No.2 indicated that the asphalt layer provided additional resistance to deformation achieved by the development of adhesive forces generated between the two layers of reed. The existence of the asphalt layer between the two layers of reed provided extra safety and the safety factor equal to 2.

An attempt is made to investigate the influence of using a second layer of asphalt spread on the top layer of reed on the overall stability of the ballast embankment. The results model test No.4 is shown in figure 5. The bearing ratio at failure $(q/c_u)_f$ is 11.4 and corresponding settlement ratios at this stress are 3.8 and 6.2 for the clay and ballast layers respectively. The overall indication in figure 5 that this additional asphalt layer had marginal influence in developing any adhesion resistance to lateral stresses along the interface between the ballast and reed layers. This may be due to the small thickness of the asphalt layer that filled parts of the pores in the crushed stone and probably coated the particles only with this film of asphalt. At working stress conditions, q/c_u=5.8 the total settlement ratio $(S/B)_T$ =3.2 and corresponding settlement ratios for clay and ballast layers being 1.96 and 1.15 respectively. The safety factor of this model (11.4/5.8) = 1.97 which is close to the value obtained from Model test No.3.

4. Safety Factors in Terms of Shear Strength

Direct shear tests were performed to determine the shear strength parameters c and ø. May occur along the interface surface of the model tests. Details are presented in table (6).

Model No.1

The interface surface consists of two materials only; the ballast particles on the top and the soft saturated clay on the bottom. Upon loading, the vertical stresses are transmitted to the soft clay layer through the interface surface. The ballast particles along the interface surface experience two types of movements, the first is a vertical movement causing the ballast particles to penetrate into the soft clay layer and the second is a lateral movement due to the developed shear stresses along the interface surface.

The determination of the generated shear stresses along the interface surface is complex; consist partly of a cohesion or adhesion component in addition to the friction component. Mohr column failure criterion is used, to simplify the analysis with assumption that adhesion is developed along the interface surface between the ballast layer and clay layer and friction is only considered between the ballast particles.

Plate 1 shows the section along the interface surface indicating the embedment of the ballast particles into the bed of soil. The plate represents the of state post failure. Where the stress ratio q/Cu ≈ 9.8 and the deformation ratio S/B=35%.

For this particular model, the bearing ratio at failure q/c_u = 5.8 obtained from figure (3). This bearing ratio corresponds to applied stress at crest level of the ballast model embankment equal to 92.16 kN/m^2. Analyzing this stress using 2:1 method revealed a vertical stress of 56.44 kN/m^2 along the interface surface between the ballast and the clay layer. The generated shear stress along the interface is then calculated using Mohr Columb failure criterion with

Adhesion component = $\alpha\ c_u$ = (0.5) (16) (Tomlinson, 1980) = 8 kN/m^2

Normal stress along the interface layer =56.44 kN/m^2

The angle internal friction ø = 42º.

The generated shear stress at failure is then calculated as:

$$\tau = \alpha.c_u + \sigma_{nf}.\tan\phi$$
$$= (0.5)(16) + 56.44 \tan 42^\circ$$
$$= 58.8\ kN/m^2$$

Figure (6) demonstrates the stresses generated along the interface surface.

Model No.2

In this model, two layers of reed were placed in reverse direction between the soft clay and the ballast layers. There are three possibilities of failure slip surface to occur as shown in figure (7).

The first is when failure occurs along the interface surface between the upper reed layer and the ballast layer, the second is when failure surface occurs between the two reed layers and the third is a failure slip surface between the lower reed layer and the soft clay layer. Due to the complexity of analyzing the state of shear stresses along these surfaces, the second case is considered only where the slip failure surface is assumed to occur between the two reed layers. The shear strength parameters obtained are shown in table (6) indicating values for both components cohesion and friction.

It is true that the reed strips are smooth and posses no cohesion or apparent cohesion, it seems that under applied vertical stress some crushing occurred in the reed bundles in the direct shear box that develops complex interaction between the two reverse reed layers upon shear, revealing some apparent cohesion c = 46.36 kN/m^2 and friction angle ø= 14.

Similar to the analysis of model No.1, the bearing ratio at failure q/Cu=9.62 revealing a vertical stress at failure 153.9 kN/m^2 at crest level of the model embankment. Analyzing the stress by 2:1 method indicates a vertical stress increment of 94.27 kN/m^2 at the interface surface. Based on Mohr Columb failure criterion and stress condition, the mobilized shear strength along the interface surface will

$\tau = \alpha . c_u + \sigma_{nf} . \tan ø$

Where adhesion = α c_u = (0.5) (16)

Normal stress = 94.27kN/m^2

Angle of internal friction = 14º

Thus the mobilized shear stress will be 69.4kN/m^2.

If the bearing ratio at failure q/c_u= 5.8 kN/m^2 from model 1 corresponding to applied stress of 92.16 kN/m^2 at crest level and 56.44 at the interface surface is considered as a working stress for all models.

Then the mobilized shear stress along the interface surface between the two layers of reed will be

$\tau = \alpha . c_u + \sigma_{nf} . \tan ø$

$\tau = 0.5*46.36 + 56.44 * \tan(14)$

$\tau = 37.25$ kN/m^2

physically this value represents the shear stresses along the interface surface between the two reed layers at normal stress 56.44 kN/m^2 in this case the safety factor S.F is calculated as 69.43/37 = 1.88.

Model No.3

In this model test asphalt layer was used between the two layers of reed along the interface surface between the ballast and the soft clay. The aim was that asphalt may provide extra resistance to the developed shear stress and ultimately provide more safety.

In this particular model four failure surfaces are expected, figure (8), the first is between the ballast layer and the top reed layer, the second between the top reed layer and the asphalt layer, the third is between the asphalt layer and the lower reed layer and the fourth is between lower reed and the soft clay layer.

The direct shear test was performed with the asphalt layer placed between the two reed layers as indicated in table (6). The direct shear test revealed shear strength parameters c = 25 kN/m^2 and angle of internal friction ø = 30.5.

The shear stress along the asphalt layer between the two reed layers under normal stress 56.44 kN/m^2 (from model) will be:

$\tau = \alpha . c_u + \sigma_{nf} . \tan ø$

$= (0.5)(2.5) + 56.44 \tan 30$
$= 33.84\ kN/m^2$

For this model test

$(q/c_u)_f = 11.81$ revealing $q_{failure} = 188.96 kN/m^2$ at crest level and interface surface $115.17\ kN/m^2$

$\tau = \alpha.c_u + \sigma nf.\tan ø$
$= (0.5)(16) + 115.17 \tan 30$
$= 74.5\ kN/m^2$

And the safety factor S.F will (75.9/34.36) = 2.21

Model No.4

In this model test two layers of asphalt were used, one between the two reed layers and one spread on the top layer of reed. Five interface failure surfaces are expected, the first is between the ballast layer and the top asphalt layer, the second between the top asphalt layer and the top reed layer, the third assumption is that the top asphalt layer and the top reed layer act as one block and the expected shear surface will be along the interface surface between top reed layer and the lower asphalt layer. The two asphalt layers and the reed layers in between are considered as one block fourth assumption is that slip surface may occur between the lower. Finely the fifth assumption for the occurrence of the expected slip surface is between soft clay layer and the lower reed layer as indicated in figure (10). With such complexity of the interaction between the layers it is extremely difficult to analyses the shear stresses as in the previous models.

5. Conclusions

The following points are drawn from the results detected from the model tests. The model test with no improvement was considered as reference of state of stresses developed along the interface.

1. Using two layers of reed in opposite direction along the interface surface provides an increase in the bearing improvement ratio 2% over the untreated condition and safety factor of 1.66.
2. Using asphalt layer is between the two layers of reed along the interface surface provides an increase in bearing improvement ratio 2.46% over the untreated condition and safety factor of 2.
3. Using two layers of asphalt, one between the two layers of reed and one spread on the top layer of reed along the interface surface provides an increase in bearing improvement ratio 2.37% over the untreated condition and safety factor of 1.97.

6. References

[1] Abbawi, Z.W.S. (2002), "Natural Materials for Soil Reinforcement" M.Sc. thesis , University of Technology, Iraq.

[2] Al-Sudani, O.A.; Daoud, D.S.; Michael, S. (1988), "Properties of particleboard from reed-type mixtures". Journal of Petroleum Research. 7(1): 197-208.

[3] Ambroziak, L. (1968). "Insulating boards from reeds and polystyrene foam. Assignee: Biuro Dokumentacji Technicznej Przemyslu Terenowego". Patent, P.N.: PL 55425, I.D.: 680620. [Polish].

[4] ASTM., "American Society for Testing and Materials", Part 14 and 19, Annual Book of ASTM Standards.

[5] ASTM D 422 – 63, (2002), "Standard Test Method for Particle – Size Analysis of Soil". Annual Book of ASTM Standards.

[6] Badanoiu, G.; Oradeanu, T. (1958). "Utilization of reed residues for particle-board manufacture with synthetic binders". Celuloza Hirtie. 7(3): 103-107. [Romanian].

[7] Bowels J.E. (1996), " Foundation Analysis and Design " 5th ed. Mc Graw-Hill book company, New York.

[8] Das B.M (2004), " Principle of foundation engineering ", 5th edition, Thomson learning Academic Resource, united states of America.

[9] Kadir, M.R.A. (1990)." Use of vegetable plants in housing construction in Northern Iraq". In: Vegetable plants and their fibres as building materials: Proceedings of the 2d international symposium sponsored by the International Union of Testing and Research Laboratories for Materials and Structures (RILEM); 1990 September 17-21; Salvador, Bahia, Brazil: 314-318.

[10] Mwasha, A.P. (2009), "Coir Fibre: A sustainable Engineering Material for the Caribbean Environment" The College of The Bahamas Research Journal, Vol.15 (2009).

[11] Terzaghi K. and Peck R.B (1967): " Soil Mechanics in Engineering Practice, " 2nd edition, John Wiley and Sons, New York.

[12] Tomlinson, M. J. (1980), " Foundation design and construction " 4th ED. London, Pitman.

[13] Wooley. G. L., (1926), "The excavation of Ur", the antiquaries Journal (6),(4).

Table (1): Section details for the four models.

Model No.	Type of test	Sketch
1	Ballast only (B)	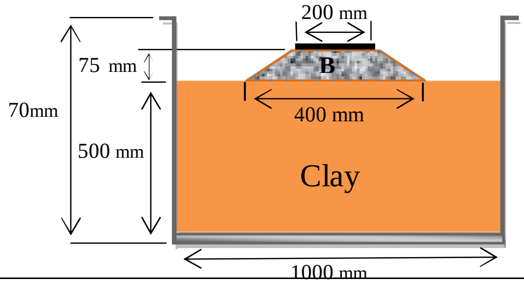
2	Ballast (B) + Two Layers of Reed (R)	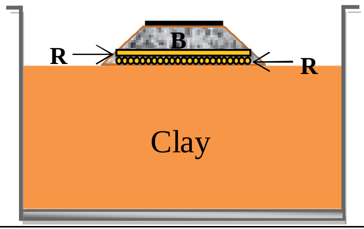
3	Ballast (B) + Two Layers of Reed (R) + Asphalt Layer in Between (A)	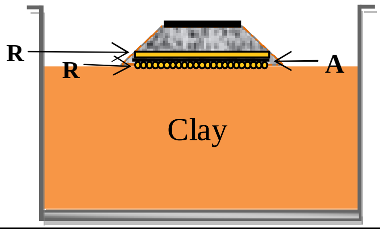
4	Ballast (B) + Two Layers of Reed (R) with Two Layers of Asphalt	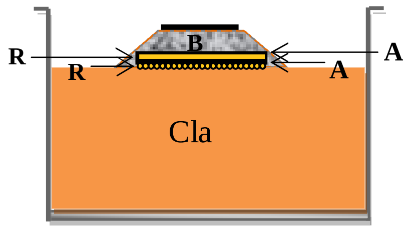

Table (2): Physical and chemical properties of natural soil used.

No.	Index property	Index value
1	Natural water content %(wc)	2.1
2	Liquid limit %(LL)	35
3	Plastic limit %(PL)	19
4	Shrinkage limit %(SL)	14
5	Plasticity index %(PI)	16
6	Activity (At)	0.45
7	Specific gravity (Gs)	2.69
8	Gravel (larger than 2mm)%	0
9	Sand (0.06 to 2mm)%	3.3
10	silt (0.005 to 0.06mm)%	31.7
11	Clay (less than 0.005mm)%	65
12	Gypsum content %	2.92
13	Total dissolved salt TDS %	4.7
14	SO3 content %	1.36
15	Organic matter O.M %	0.44
16	PH value	8.9
17	Soil symbols (USCS)	CL

Table (3): Physical properties of the crushed stone used.

No.	Index property	Index value
1	Max. dry unit weight (kN/m3)	15.7
2	Min. dry unit weight (kN/m3)	13.5
3	D10 (mm)	4.66
4	D30 (mm)	5.0
5	D60 (mm)	5.12
6	Specific gravity (Gs)	2.64
7	Coeff. of uniformity (Cu)	1.02
8	Coeff. of curvature (Cc)	1.05
9	Relative density (Dr%)	71
10	Angle of internal friction (f^0) at Dr = 71%	42

Table (4): Physical properties of the asphalt cement used.

No. of Test	Type of test	Unit	Result
1	Penetration (25C°, 100gm, 5 sec.)ASTM D 5 - 83	1/10mm	46
2	Ductility (25C°, 5 cm/min)ASTM 36 -70	Cm	> 150
3	Softening Point (Ring and Ball) (0 C° /min.) ASTM D 36-70	C°	49.5
4	Specific gravity at 25C°/25C° ASTM D 70 - 82	-	1.038

5	Flash Point (Cleave land open cup)ASTM D 92 - 62	C°	310
6	Fire Point (Cleave land open cup)	C°	334
7	Kinematics Viscosity at 135C°ASTM D 2170 - 83	centistoke	598
8	Loss on Heat at (163c°, 50gm, 5hrs.)ASTM D 1754 - 83	%	0.535
9	Penetration of Residue % of original penetration at 25C°ASTM D 1745 - 83	1/10 mm	43.5
10	Ductility of Residue at (25C°, 5cm/min.)ASTM D 1754 -83	cm	86

Table (5): Settlement Ratio at Working Stress Ratio q/c_u = 5.8

No. of Model	Type of test	Sketch	c (kPa)	Ø(deg.)
1	Ballast only	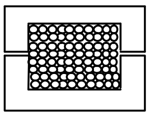	0	42
2	Reed without asphalt	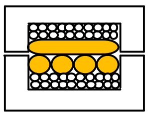	46.36	14
3	Asphalt is between the layers of reed	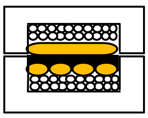	2.5	30

Table (6): Shear strength parameters from direct shear test.

Model NO.	Type of test	(S/B)Total	(S/B)Clay	(S/B)Ballast	S.F
1	Ballast only	10	1.98	8	1.0
2	Reed without asphalt	4.9	2.0	2.9	1.66
3	Asphalt is between the layers of reed	3.0	2	1	2.0
4	Asphalt is between and above the layers of reed	3.2	1.95	1.15	1.97

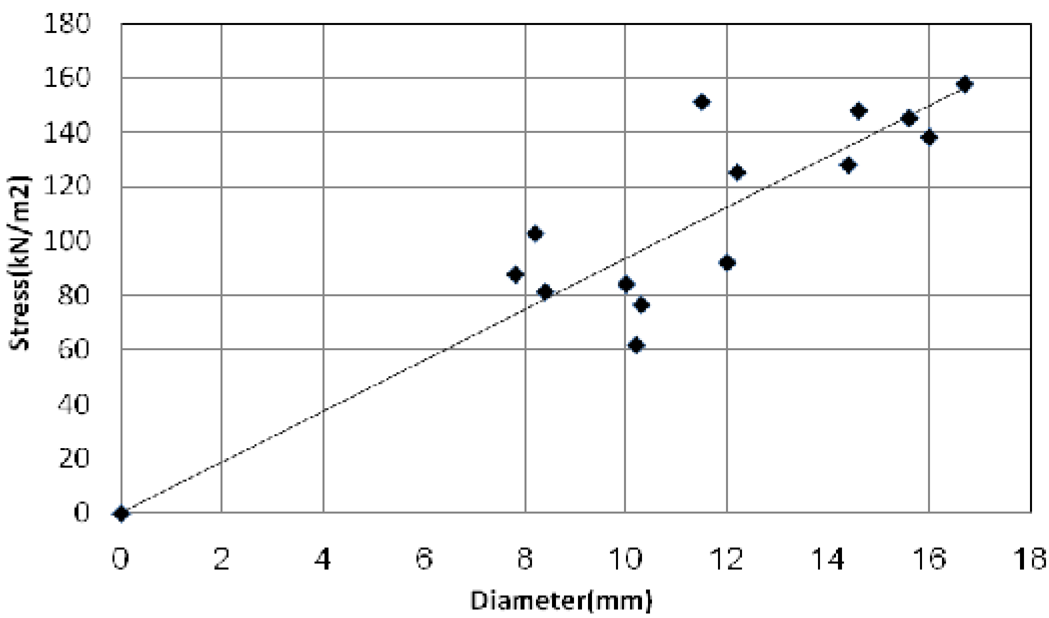

Figure (1): Variation of stress with diameter of reed.

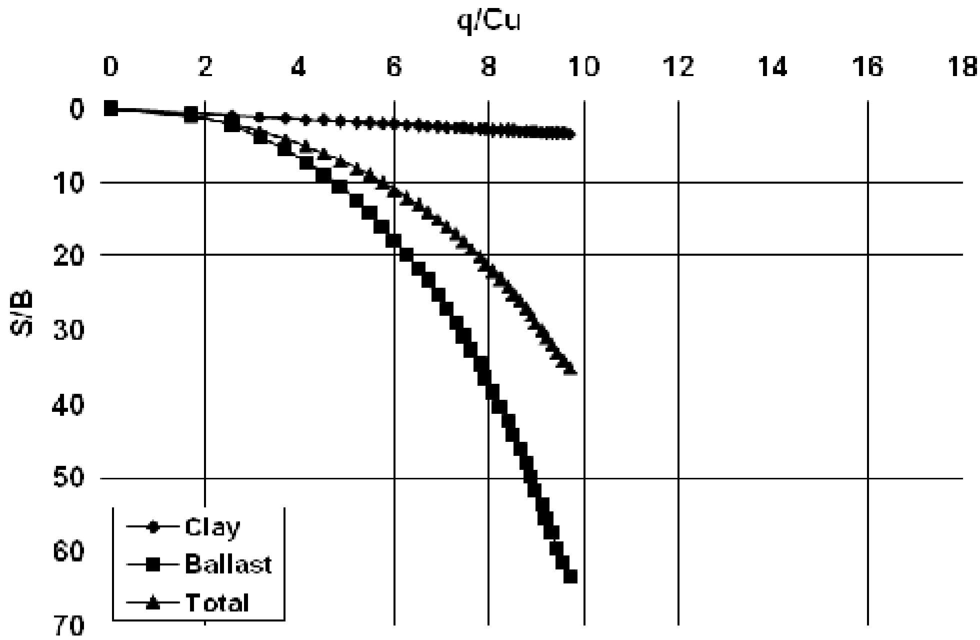

Figure (2): Relationship between bearing ratio (q/c_u) and deformation ratio (S/B)% for ballast only

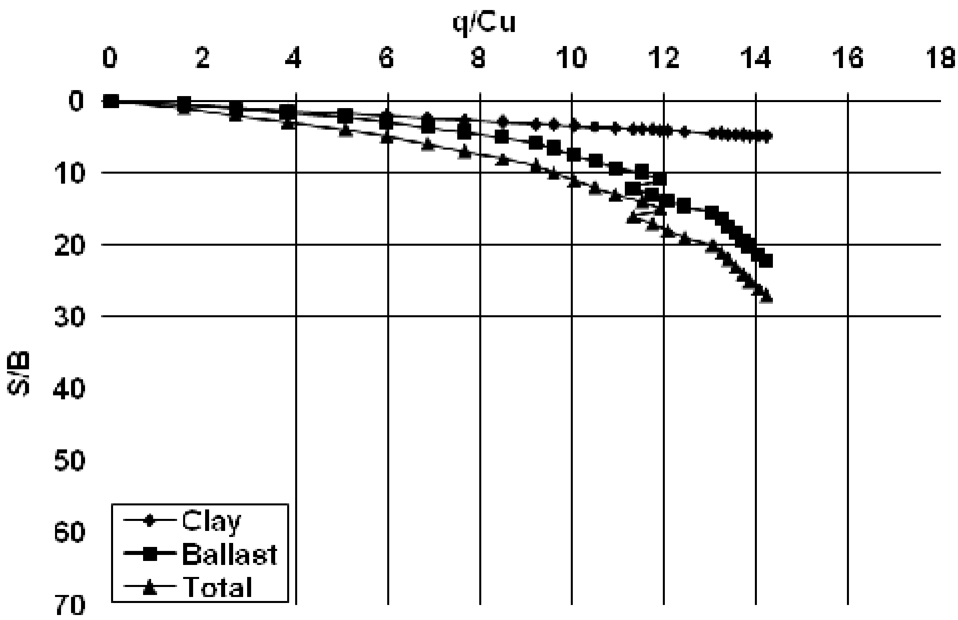

Figure (3): Relationship between bearing ratio (q/c_u) and deformation ratio (S/B)% for reed without asphalt

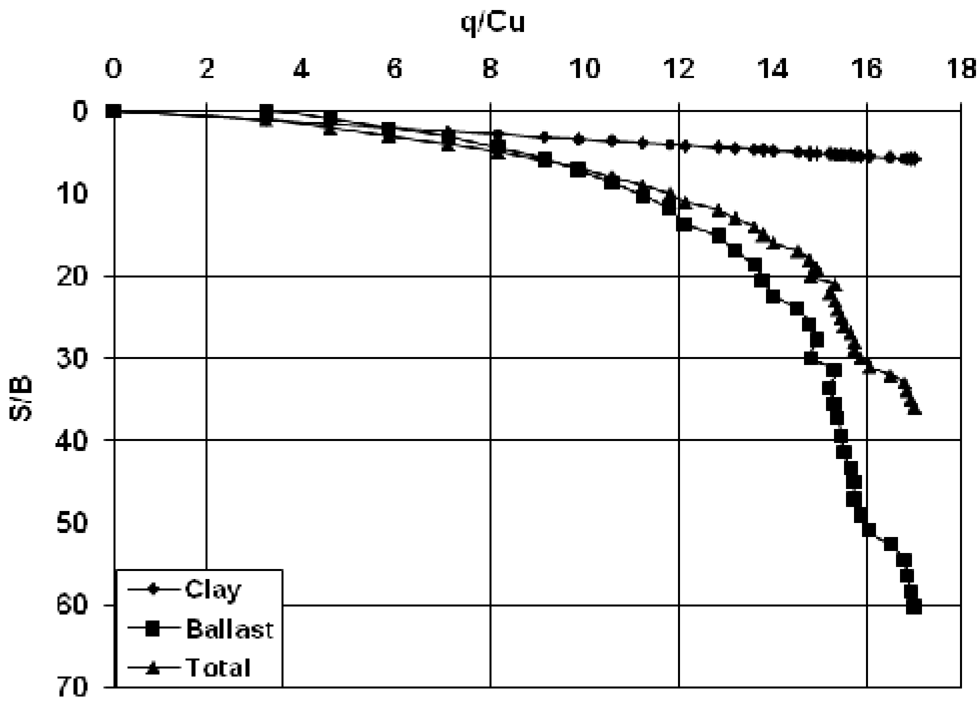

Figure (4): Relationship between bearing ratio (q/c_u) and deformation ratio (S/B)% for asphalt is between the layers of reed

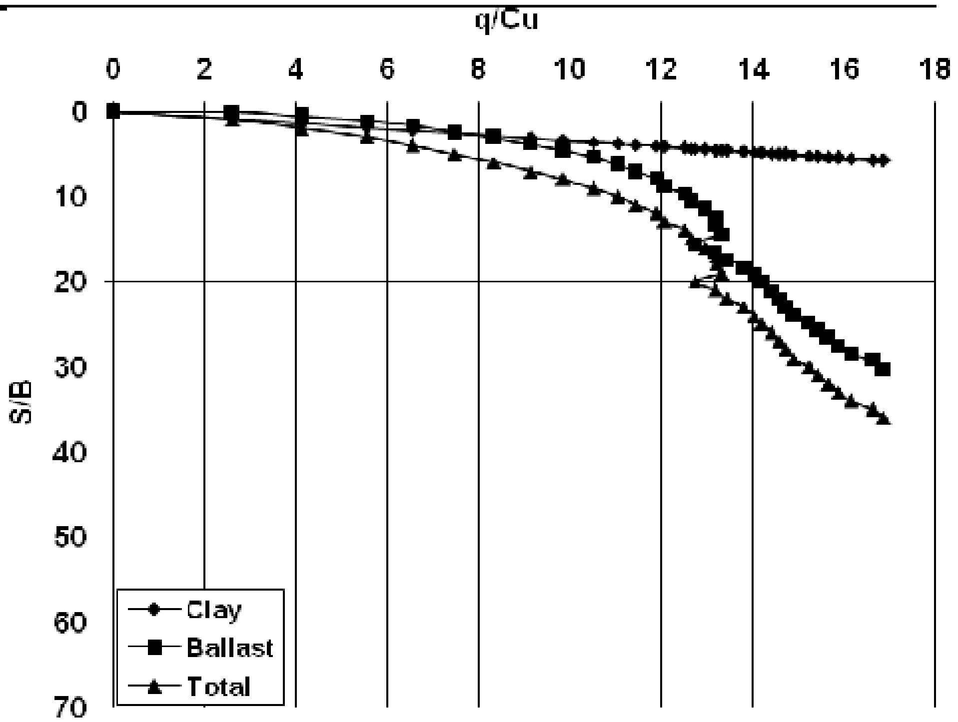

Figure (5): Relationship between bearing ratio (q/c_u) and deformation ratio (S/B)% for asphalt is between and above the layers of reed

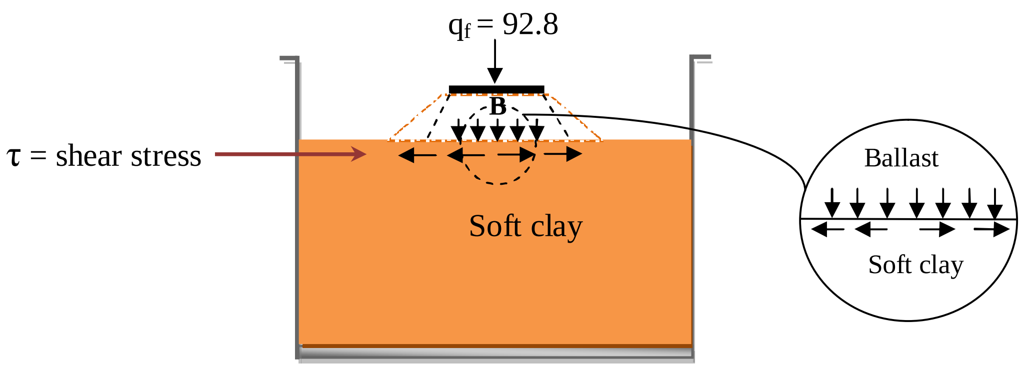

Figure (6): Cross section of model no. 1

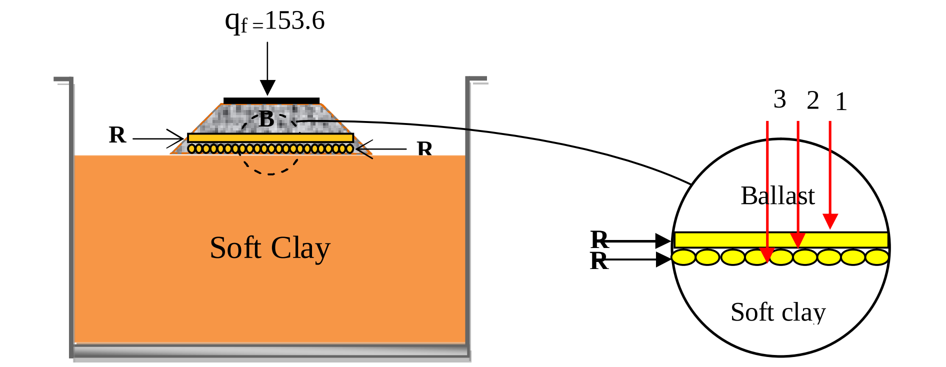

Figure (7): Cross section of model no. 2

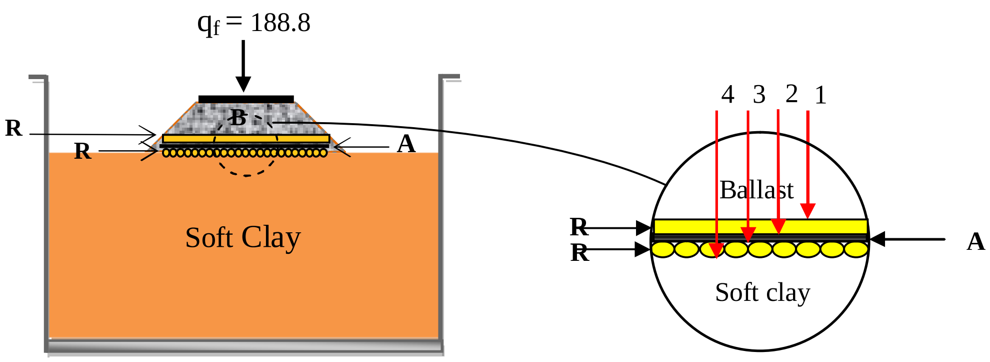

Figure (8): Cross section of model no. 3

Figure (9): Model no.3 after the test

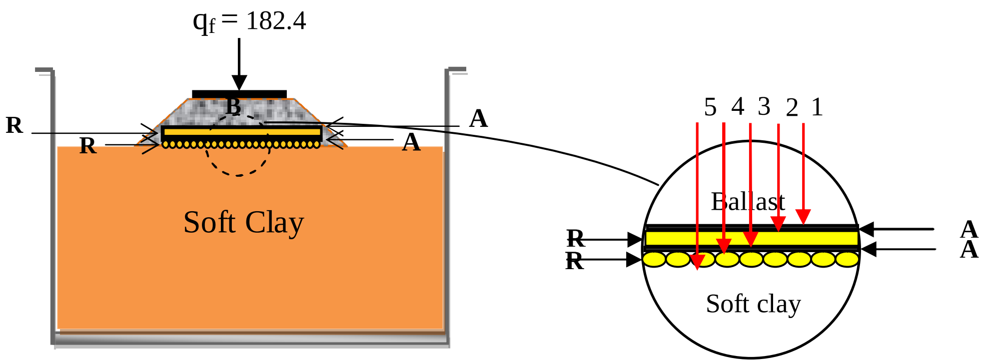

Figure (10): Cross section of model no. 4

Figure (11): Model no.4 after the test